

Observation of Higher Order Facets on ^3He Crystals

V. Tsepelin, H. Alles, A. Babkin,* J. P. H. Härme, R. Jochemsen,[†] A. Ya. Parshin,[‡] and G. Tvalashvili[§]

Low Temperature Laboratory, Helsinki University of Technology, P.O. Box 2200, FIN-02015 HUT, Finland

(Received 12 October 2000)

Faceting has been observed on ^3He crystals investigated with a low-temperature Fabry-Pérot interferometer. Nine types of facets were clearly identified during growth of a bcc- ^3He single crystal at a temperature of 0.55 mK, while previously only three types of facets have been seen. Because of the weak coupling between the liquid-solid interface and the solid lattice in ^3He the facets are apparently too small to be observed in equilibrium. The number of facets observed in our experimental conditions is consistent with the theory of dynamic roughening.

DOI: 10.1103/PhysRevLett.86.1042

PACS numbers: 67.80.-s, 68.08.-p, 68.35.Rh, 81.10.Aj

In equilibrium, the surface of crystalline matter can be in two principally different states, either smooth (faceted) or rough (rounded) according to its crystallographic orientation and temperature. The phase transition between these two surface states at the so-called roughening temperature is generally expected to be of the Kosterlitz-Thouless type [1]. According to theory, the crystal surface is expected to undergo a sequence of roughening transitions, each type of facet having its own transition temperature. So at low temperature the equilibrium crystal shape should show many different types of facets.

Experimentally, however, this situation is very difficult to achieve. Almost no crystal can reach its equilibrium shape, mostly for kinetic reasons: the diffusion on the solid surface in equilibrium with the vapor is much too slow in the temperature region of the roughening transition. Nevertheless, some facets and roughening transitions for facets with mostly low Miller indices have been observed in microscopic metal crystals [2,3], in some organic crystals [4], and in ice crystals [5]. So it was quite a surprise that recently more than 60 different types of facets were seen at room temperature on a lyotropic liquid crystal, even revealing the long expected “devils’s staircase” [6]. The appearance of vicinal facets with large Miller indices in this system was explained by the coincidence of quite large surface tension and interplanar distance with an exceptionally low elastic modulus.

In ^4He where zero-point motion is large (a quantum crystal) and the liquid is superfluid, a unique situation arises. The crystal shape can be followed along the melting curve from about 2 K down to $T = 0$. Below 1.5 K, the growth dynamics is very fast. Nevertheless, even down to $T = 2$ mK not more than 3 types of facets have yet been seen, with their roughening transitions at $T = 1.3$ K, 0.9 K, and 0.36 K [7,8].

For both ^4He and ^3He the coupling of the interface to the solid (lattice) is assumed to be so weak that it results in a very small size of equilibrium facets, often too small to be observed [9]. Thus the equilibrium crystal shape should look rounded even if a lot of higher order facets

exist. However, faceted areas grow slower than rough areas, resulting in growth-induced completely faceted crystal shapes, and one is tempted to search for larger facets by observing the crystal during its growth. On the other hand, crystal growth has the effect of displacing the roughening transition to lower temperatures [10,11]. So how many different types of facets can one observe on the surface of a crystal?

In this Letter, we present evidence for the observation of altogether nine different types of facets when growing ^3He single crystals at a temperature of 0.55 mK. In some instances we even see a series of 4 consecutive facets, forming a precursor of a “devil’s staircase.” Note that the facets (110), (100), and (211) have been observed before on ^3He crystals [12,13].

Our experimental setup was designed for studies of morphology and growth kinetics of ^3He crystals. The cryostat has all optical components inside the 4-K vacuum can with the exception of a He-Ne laser located at room temperature [8]. The heart of our optical system is a Fabry-Pérot multiple-beam interferometer with a phase-shift facility [14,15]. The operating temperature of the interferometer is close to 10 mK, which makes it probably the coldest multiple-beam interferometer ever made. Path interferometry has the advantage of a low required light intensity [16] and allowing simultaneous observation of the global crystal shape and of the fine details of the solid/liquid interface. The vertical resolution in the interface position is a few μm , while the horizontal resolution of about 15 μm is limited by the pixel size of the slow-scan CCD camera sensor.

All crystals under study were single crystals nucleated from the B phase of superfluid ^3He [17]. The ^3He crystals were grown and melted by pressure changes at our lowest temperature of 0.55 mK, where the latent heat of solidification is very small. The temperature was determined from the equilibrium melting pressure, which was measured with a high precision Straty-Adams strain gauge [18] with a resolution of a few μbars at 35 bars. The heat input to the cell due to a 20 ms pulse of the He-Ne

laser ($\lambda = 632.8$ nm) is less than 0.1 nJ, and the maximum pulse rate of one pulse per 4 sec is limited by the readout rate of the CCD controller.

Figure 1 shows an interferogram of a ^3He single crystal at 0.55 mK during growth. The crystal lies in the center of the interferogram; the several regions with equidistant parallel fringes correspond to flat planes (facets) on the crystal surface. At the top left and bottom the background pattern is visible. It arises from the liquid helium wedge (due to the 2° tilt of the upper window) and the nonparallelism of the mirrors. The field of view is a circle with a diameter of about 8 mm.

All the facets were visible at a certain growth rate; when the growth was stopped the facets decreased and the crystal became more round on a time scale of tens of seconds. The initial size of the facets appears to be mainly determined by the shape of the crystal just before it starts growing. When growth continues, the slowly growing densely populated facets (110) and (100) determine more and more the shape of the crystal. We identified the type of each facet on the crystal surface by comparing the measured angles between facets with the theoretically possible ones for the perfect bcc structure. This justifies us in neglecting entirely the relative sizes of the crystal facets. Two different approaches were utilized: a phase-shift technique was applied when a crystal was under stable conditions [14] and intensity based analysis methods were used in dynamic situations [19].

The phase-shift technique yields a simple and reliable measurement of the wavefront phase, which is directly proportional to the thickness of the crystal [14,20]. When the thickness at each point is known the angles between different facets can be calculated directly. With intensity based analysis we resolved the crystal surface structure from the interferograms recorded during crystal growth. The parameters of the facets were obtained with the assumption

that fringes belonging to the same facet are parallel and equidistant. To determine the fringes accurately the positions of the minima (maxima) were located and combined to a skeleton pattern. The distance between parallel lines and their slope was then calculated using a Hough transform [21], from which the facet orientation can be uniquely determined.

The shape of the ^3He crystal shown in Fig. 1 was resolved using the intensity based method with the corresponding skeleton pattern presented in Fig. 2. The white dashed-line polygons mark the edges of the identified facets and the Miller indices indicate the type of each facet. All identified facets have been detected on more than one interferogram, and at least three equally spaced parallel fringes were observed for each facet. The typical difference between the expected and measured angles was up to 2° ; in the worst cases it was around 6° for the shortest fringes.

Of course one can find a large number of facets which are infinitely close to each other and satisfy the selection criteria within experimental precision. The planes which are most likely to appear as external facets are the ones with the highest reticular density, which is directly proportional to the interplanar spacing d_{hkl} of a given type of plane. In the bcc lattice $d_{hkl} = \frac{1}{2}a(h^2 + k^2 + l^2)^{-1/2}$. For Fig. 1 and all other interferograms we have always chosen the most "stable" facets consistent with the experimentally determined angles. Table I shows all the observed facets at 0.55 mK. Figure 3 shows the positions of these facets on one elementary patch of the whole crystal habit. Also the positions of those facets which were not observed, but have a higher (or equal) reticular density and thus a higher (or equal) roughening temperature than the (510) plane, are shown in Fig. 3 as open circles.

Of particular interest is the question: how many different types of facets can be observed at a given temperature

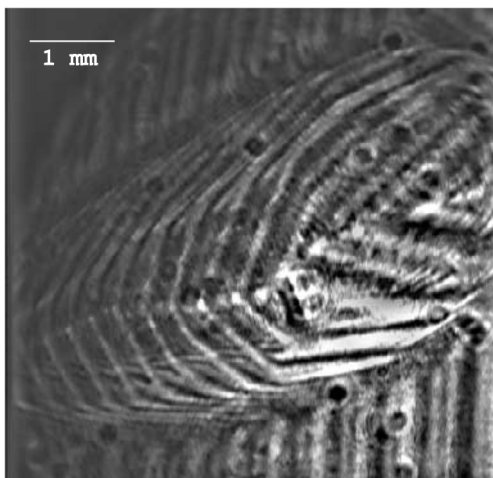


FIG. 1. The interferogram of a growing ^3He single crystal at 0.55 mK. The regions with equidistant parallel fringes correspond to flat surfaces.

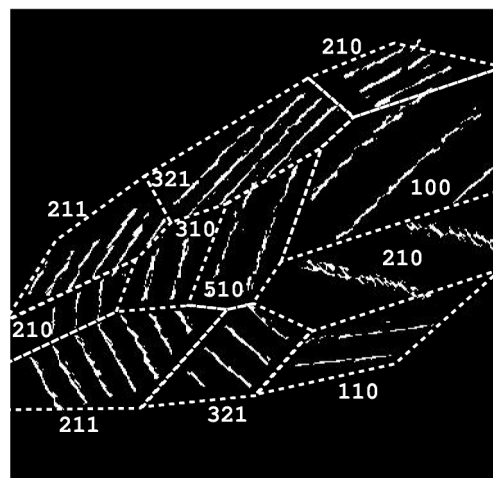


FIG. 2. The skeleton pattern of the crystal in Fig. 1. White dashed lines indicate the edges of the identified facets with the corresponding Miller indices.

TABLE I. Miller indices of the experimentally observed types of facets, their reciprocal lattice vectors $\langle hkl \rangle$, the interplanar distance ratio with respect to the (110) facet, and the highest temperature $T_{\text{obs}}^{\text{max}}$ at which the facet has been observed.

| Miller index | $\langle hkl \rangle$ | $(d_{110}/d_{hkl})^2$ | $T_{\text{obs}}^{\text{max}}$ (mK) | Refs. |
|--------------|---|-----------------------|------------------------------------|-------|
| 110 | $\langle \frac{1}{2} \frac{1}{2} 0 \rangle$ | 1 | 100 | [12] |
| 100 | $\langle 100 \rangle$ | 2 | 10 | [13] |
| 211 | $\langle 1 \frac{1}{2} \frac{1}{2} \rangle$ | 3 | <10 | [13] |
| 310 | $\langle 1 \frac{1}{2} \frac{1}{2} 0 \rangle$ | 5 | 0.55 | |
| 111 | $\langle 111 \rangle$ | 6 | 0.55 | |
| 321 | $\langle 1 \frac{1}{2} 1 \frac{1}{2} \rangle$ | 7 | 0.55 | |
| 411 | $\langle 2 \frac{1}{2} \frac{1}{2} \rangle$ | 9 | 0.55 | |
| 210 | $\langle 210 \rangle$ | 10 | 0.55 | |
| 510 | $\langle 2 \frac{1}{2} \frac{1}{2} 0 \rangle$ | 13 | 0.55 | |

and at a given growth rate? In the following, the possible number and the size of facets in equilibrium will be discussed, and then the effect of dynamic roughening is considered.

The roughening transition temperature T_R of a particular facet is given by

$$k_B T_R = \frac{2}{\pi} \sqrt{\gamma_{\parallel} \gamma_{\perp}} d^2, \quad (1)$$

where k_B is the Boltzmann constant, d the interplanar distance (height of the elementary step on the facet), and γ_{\parallel} and γ_{\perp} the principal components of the surface stiffness for that surface [1,10]. Both components of γ should be measured at a temperature above but close to the expected transition temperature for that part of the surface. The surface stiffness of ^3He crystals has been measured only at rather high temperatures [22], where no facets exist and γ is almost isotropic and temperature independent, $\gamma = \gamma_0 \approx 0.06 \text{ erg/cm}^2$. In principle at low temperatures γ becomes strongly anisotropic for vicinal surfaces,

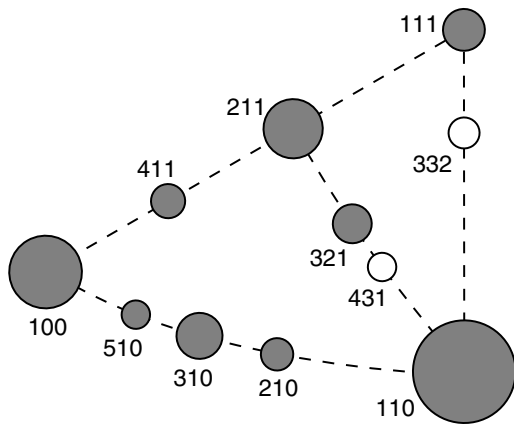


FIG. 3. Diagram with the Miller indices of facets in the bcc structure of ^3He . Filled points represent experimentally observed facets, empty ones correspond to facets expected to be seen. The diameter of the circles is proportional to the interplanar distance. The coordinates are exact, looking along the [111] direction.

which are tilted by a small angle with respect to one of the “primary” facets, and which may be viewed as a distribution of terraces and steps [10,23]. However, since the step width on the helium interface is very large due to the weak coupling (the width is about $10\times$ the lattice constant in ^4He [24], and is expected to be even larger in ^3He due to the larger zero point fluctuations [9,22]), only surfaces with very large Miller indices may be called vicinal. So the roughening transition causes a change of the surface characteristics only in very close vicinity to a facet. To estimate the total number of facets in equilibrium at a given temperature we may thus assume $\gamma_{\parallel} = \gamma_{\perp} = \gamma_0$ [25]. Among the observed facets Eq. (1) gives the lowest T_R for the (510) type, with $T_{510} \approx 20 \text{ mK}$, and more than 1000 different types of facets should exist in equilibrium at 0.55 mK.

In ^3He in equilibrium facets are apparently too small to be observed directly, even the most “stable” (110) ones [12,13,22]; the newly observed facets should be even smaller. Indeed, as was first shown by Landau [26], the equilibrium size of any facet L_{hkl} is proportional to β_{hkl} , $L_{hkl} \approx \beta_{hkl} R / (d_{hkl} \gamma_0)$, where R is a characteristic size of the crystal, and β_{hkl} is the step free energy. In the absence of direct experimental data on the values of β , we try to make a rough estimate of them, including those for higher order facets. In the weak coupling approximation [10], $\beta \sim d\sqrt{\gamma V}$, where V is the energy barrier, which pins a liquid-solid interface to the crystal lattice and separates neighboring equilibrium positions of the interface. If the effective width of the interface l is large, V is exponentially small (weak coupling) [10]. Assuming that l is approximately the same for all surface orientations, we may write $V \sim \gamma \exp(-l/d)$ and

$$\beta \sim d\gamma \exp(-l/2d). \quad (2)$$

There is no direct experimental data on l in ^3He nor in ^4He . However, we can calculate l in ^4He , using Eq. (2) and the known values of $\beta = 4.2 \times 10^{-10} \text{ erg/cm}$ [23] and $\gamma = 0.245 \text{ erg/cm}^2$ [9] for (1000) facets. The result is $l/d_{1000} = 2.5$ [27]. In ^3He we expect a somewhat larger value, so it is reasonable to assume $l/d_{110} = 3-4$. For facets like (411), (210), (510), it gives $L \approx (10^{-2}-10^{-3})R$. With our resolution (we need three fringes to determine a facet) it is hardly possible to observe such small facets.

We see that, most probably, direct observation of new facets is only possible rather far from equilibrium, in a course of sufficiently rapid growth. However, under these conditions some facets may disappear due to dynamic roughening [10,11]. The typical chemical potential difference sufficient to destroy a facet at a temperature well below corresponding T_R can be estimated as

$$\delta\mu \approx \frac{\beta^2}{\gamma d^3}. \quad (3)$$

For the facet (510), which has the lowest roughening temperature of all the observed facets, Eq. (3) with $l/d_{110} = 3$ gives a related overpressure $\delta p \approx 3$ mbar. This is close to the value used in our measurements (5 mbar maximum). Despite the uncertainties in our approximation we may conclude that under our experimental conditions dynamic roughening really can limit the observation of new facets. At lower growth rates possibly more facets would be present on the crystal shape, but they would be too small for us to observe.

To summarize, ^3He single crystals were grown and studied at a temperature of 0.55 mK using a state-of-the-art multiple-beam interferometer. Using advanced digital image processing techniques, altogether nine facet types were identified during crystal growth with an appropriate overpressure. This result is consistent with theoretical estimates of the number of facets at this temperature, taking into account the suppression due to dynamic roughening. It is also clear that direct measurements on the growth kinetics of different facets are needed. Finally, we like to point out the striking difference with ^4He , where until now only three types of facets have been seen. Could this be caused by the difference in crystal structure (hcp vs bcc)? Or has one not searched properly?

We would like to thank A. Andreev, S. Balibar, P. Hakonen, K. Keshishev, and E. Thuneberg for help and useful discussions. One of us (R.J.) would like to thank the Low Temperature Laboratory for warm hospitality during several visits. This work was supported by the ULTI II (ERB FMGE CT98 0122) and ULTI III (HPRI-1999-CT-00050) grants of the European Union and the Academy of Finland [Finnish Centre of Excellence Programme (2000-2005)] and by INTAS Grant No. 96-610.

*Present address: Department of Physics and Astronomy, University of New Mexico, 800 Yale Boulevard N.E., Albuquerque, NM 87131.

†Permanent address: Kamerlingh Onnes Laboratory, Leiden University, P.O. Box 9504, 2300RA Leiden, The Netherlands.

‡Permanent address: P.L. Kapitza Institute for Physical Problems, ul. Kosygina 2, 117334 Moscow, Russia.

§Present address: Department of Physics, Lancaster University, Lancaster LA1 4YB, U.K.

- [1] D.S. Fisher and J.D. Weeks, Phys. Rev. Lett. **50**, 1077 (1983).
- [2] J.C. Heyraud and J.J. Métois, J. Cryst. Growth **82**, 269 (1987).
- [3] J. Lapujoulade, J. Perreau, and A. Kara, Surf. Sci. **129**, 59 (1983).
- [4] See S. Balibar and P. Nozières, Solid State Commun. **92**, 19 (1994), and references therein.
- [5] M. Elbaum, Phys. Rev. Lett. **67**, 2982 (1991).
- [6] P. Pieranski *et al.*, Phys. Rev. Lett. **84**, 2409 (2000).
- [7] P.E. Wolf, S. Balibar, and F. Gallet, Phys. Rev. Lett. **51**, 1366 (1983).
- [8] J.P. Ruutu *et al.*, J. Low Temp. Phys. **112**, 117 (1998).
- [9] S. Balibar *et al.*, Physica (Amsterdam) **169B**, 209 (1991), and references therein.
- [10] P. Nozières, in *Solids Far From Equilibrium*, edited by C. Godrèche (Cambridge University Press, Cambridge, England, 1991).
- [11] P. Nozières and F. Gallet, J. Phys. (Paris) **48**, 353 (1987).
- [12] E. Rolley, S. Balibar, and F. Gallet, Europhys. Lett. **2**, 247 (1986).
- [13] R. Wagner *et al.*, Phys. Rev. Lett. **76**, 263 (1996); R. Wagner, Ph.D. thesis, Leiden University, 1995.
- [14] J.P.H. Härme *et al.*, Physica (Amsterdam) **284B–288B**, 349 (2000).
- [15] V. Tsepelin *et al.* (to be published).
- [16] P. Hakonen *et al.*, J. Low Temp. Phys. **101**, 41 (1995).
- [17] V. Tsepelin *et al.*, Physica (Amsterdam) **284B–288B**, 351 (2000).
- [18] G.C. Straty and E.D. Adams, Rev. Sci. Instrum. **40**, 1393 (1969).
- [19] D.W. Robinson and G.T. Reid, *Interferogram Analysis* (IOP Publishing, Ltd., Bristol, 1993).
- [20] G. Bönsch and H. Böhme, Optik **82**, 161 (1989).
- [21] J. Illingworth and J. Kittler, Comput. Vis. Graph. Image Process. **44**, 87 (1988).
- [22] E. Rolley *et al.*, Europhys. Lett. **8**, 523 (1989).
- [23] E. Rolley *et al.*, J. Low Temp. Phys. **99**, 851 (1995).
- [24] S. Balibar, C. Guthmann, and E. Rolley, J. Phys. **3**, 1475 (1993). See also V. Tsepelin *et al.*, Phys. Rev. Lett. **83**, 4804 (1999).
- [25] In the weak coupling approximation, which is expected to be valid in ^3He as well as in ^4He , the renormalization of γ near T_R due to critical fluctuations results in a rather small correction in T_R (see Refs. [10,11]).
- [26] L.D. Landau, *Collected Papers* (Pergamon Press, Oxford, 1971).
- [27] See also F. Pederiva *et al.*, Phys. Rev. Lett. **72**, 2589 (1994), who find $l/d \approx 4$ in ^4He with a variational Monte Carlo simulation of the solid-liquid interface. Unfortunately, the calculation is done only for the (100) surface of the fcc structure.